

# REPORT DOCUMENTATION PAGE

Form Approved  
OMB NO. 0704-0188

Public Reporting burden for this collection of information is estimated to average 1 hour per response, including the time for reviewing instructions, searching existing data sources, gathering and maintaining the data needed, and completing and reviewing the collection of information. Send comment regarding this burden estimates or any other aspect of this collection of information, including suggestions for reducing this burden, to Washington Headquarters Services, Directorate for Information Operations and Reports, 1215 Jefferson Davis Highway, Suite 1204, Arlington, VA 22202-4302, and to the Office of Management and Budget, Paperwork Reduction Project (0704-0188,) Washington, DC 20503.

1. AGENCY USE ONLY (Leave Blank)		2. REPORT DATE 5/3/01		3. REPORT TYPE AND DATES COVERED Final report; end date 31 Aug 00 18 Nov 96-	
4. TITLE AND SUBTITLE Infrared Spectroscopy of a Hyper-Velocity Shock				5. FUNDING NUMBERS  Contract DAAG55-97-1-0003	
6. AUTHOR(S)  Peter Erdman					
7. PERFORMING ORGANIZATION NAME(S) AND ADDRESS(ES)  Embry-Riddle Aeronautical University; Daytona Beach, FL				8. PERFORMING ORGANIZATION REPORT NUMBER	
9. SPONSORING / MONITORING AGENCY NAME(S) AND ADDRESS(ES)  U. S. Army Research Office P.O. Box 12211 Research Triangle Park, NC 27709-2211				10. SPONSORING / MONITORING AGENCY REPORT NUMBER  36611.1-EG-SD1	
11. SUPPLEMENTARY NOTES The views, opinions and/or findings contained in this report are those of the author(s) and should not be construed as an official Department of the Army position, policy or decision, unless so designated by other documentation.					
12 a. DISTRIBUTION / AVAILABILITY STATEMENT  Approved for public release; distribution unlimited.				12 b. DISTRIBUTION CODE	
13. ABSTRACT (Maximum 200 words)  We have continued the investigation of hypervelocity shocks that began with the highly successful Bowshock I and II atmospheric sounding rocket experiments. Instruments aboard those vehicles performed measurements of the ultraviolet and vacuum ultraviolet emission excited in the high temperature gas produced by the shock ahead of the hypervelocity body. We have developed the experimental techniques and the instruments necessary to expand those earlier experiments into the infrared portion of the spectrum where ground-state, molecular, ro-vibrational emission can be observed as the most direct measure of shock temperatures.  With this project's support, we have defined, designed and nearly completed the construction of the hypervelocity shockwave experiment that has come to be known as "DEBI". The flight instrumentation originally proposed has made some evolutionary changes as a result of new thoughts on the spectral regions to emphasize, detector developments, and background suppression techniques that should greatly improve the infrared measurements.					
14. SUBJECT TERMS				15. NUMBER OF PAGES 14	
				16. PRICE CODE	
17. SECURITY CLASSIFICATION OR REPORT UNCLASSIFIED	18. SECURITY CLASSIFICATION ON THIS PAGE UNCLASSIFIED	19. SECURITY CLASSIFICATION OF ABSTRACT UNCLASSIFIED	20. LIMITATION OF ABSTRACT  UL		

NSN 7540-01-280-5500

Standard Form 298 (Rev.2-89)  
Prescribed by ANSI Std. Z39-18  
298-102

20010516 113

## Synopsis of Work:

Optical diagnostic instrumentation aboard high-speed, atmospheric, sounding rockets has proven to be a very successful way of investigating hyper-velocity shocks. The intensely heated air in the shock produces optical radiation from both atomic and molecular species over a wide spectrum. This radiation is characteristic of the shock conditions, and can be used to derive temperatures and species densities in the shock region. The Bowshock I and II experiments concentrated on the shorter wavelength regions of such emission, specifically the ultraviolet emission due mostly to nitric oxide and OH, and the vacuum ultraviolet emission due to atomic nitrogen, hydrogen and oxygen. Modeling of these emissions has proven to be a challenging task, and it is now clear that measurements in other portions of the spectrum would be important to validate the conclusions of these models. The number of data points is at present very small, and without such validation it is not yet clear what power of prediction exists for other, unmeasured conditions.

These experiments were characterized by a close collaboration between the experimental and modeling teams, which was essential for the objective--better understanding of the shock characteristics including temperatures, densities, and species composition. The net result was a data set and modeling evolution that has proven its usefulness in improving our understanding of this phenomenon. In order to continue this valuable process, new measurements must be made in order to test the models as they exist at their present state of evolution, and to provide insights into how they might be improved.

Moving our observations into the infrared, we can observe emission from ground state molecules that are part of the ambient atmosphere, in addition to those that are created in the shock chemistry. This becomes a powerful test of the models' ability to predict the shock "temperatures". For example, if the vibrational temperature of nitric oxide created in the shock was first fit by ultraviolet observations of the Gamma bands, then that same temperature should apply to ground state ro-vibrational emission observed in the infrared from the nitric oxide fundamental band or its overtones. Similarly, the carbon dioxide fundamental or its overtones could be observed and vibrational temperatures compared with those of nitric oxide. Hydroxyl excited state emission observed in the ultraviolet also has ground state ro-vibrational bands in the infrared as a further check on this process.

We have defined, designed, and have nearly completed the construction of a suitable set of instruments to fly on a sounding rocket that will nearly duplicate the altitude and velocity regime of the Bowshock I experiment. These instruments include ultraviolet photometers, infrared radiometers, and a scanning IR spectrometer. As on the previous Bowshock experiments, we will be viewing not only in the forward direction, directly at the stagnation point, but also at an angle to the velocity vector.

All the instruments will also have their input from fiber optics running between their respective entrance apertures and the appropriate windows. For the UV measurements on BSI & II, quartz fibers worked well, but do not transmit far enough into the IR. Fortunately, there does exist a new fluoride glass fiber material with excellent transmission out to nearly 5 microns. Hence the location of the instruments can be separated from their viewing geometry requirements, without which it would be impossible to fit even this instrument set into the very small payload package.

It is impossible to fit all the desirable instrumentation into any payload with such limited resources, or even to use conventional designs for them. We believe that the instrument suite described below presents a good compromise of measurement coverage and practicality for this flight. An AIAA paper describing this payload is included.

## **Optical Instrumentation Overview:**

### **UV filtered photometers – Two Channels**

- One channel in each look direction
- $\sim 0.24\mu$  band center
- Photomultiplier detectors, pulse counting only

### **Micro Optic Multispectral Radiometer (MOMS) – Fourteen Channels**

- Eight channels of MWIR ( $3\text{--}4.3\mu$  wavelength)
- Six channels of SWIR ( $1.0\text{--}2.7\mu$  wavelength)

### **Scanning IR Spectrometer ( $1.0 - 3.0\mu$ ) – Sixteen Channels**

- Dual Look Direction
- Eight Detector Channels in each look direction

### **Look Directions:**

- One spectrometer input and one UV photometer looking forward at stagnation point through recessed window in nose piece
- Second spectrometer input, second UV photometer, and all IR MOMS channels observing sideways through two recessed windows located as far forward on nose piece as practical

## **Instrument Specifics:**

### **Two UV filtered photometers**

Inputs coupled to windows with UV silica fibers.

Side-looking fiber area 10x that of forward-looking fiber for maximum dynamic range in signal levels

~240nm band center, ~50nm filter bandpass (FWHM)

Photomultiplier detectors, CsTe cathode—very low noise and “solar blind”

Detector pulse counting outputs integrated with 20 bit counters

“Legacy” data for overlap with BSI & II

### **Fourteen IR MOMS Radiometers**

Eight channels of MWIR (3--4.3 $\mu$  wavelength)

Six channels monitoring 3-4 $\mu$  region with 0.2 $\mu$  spacing, ~0.2 $\mu$  filter bandpass

One channel ~4.3 $\mu$  band center for CO<sub>2</sub>, ~0.2 $\mu$  filter bandpass

One channel ~0.8 $\mu$  filter bandpass centered at ~3.5 $\mu$  for maximum sensitivity.

Six channels of SWIR (1.0—2.7 $\mu$  wavelength)

Provide: spectrometer backup (as on BSI & II), high temporal resolution, high sensitivity

Place filter bandcenters at emission peaks and predicted “holes”

(2.7 $\mu$  CO<sub>2</sub>, NO; 2.3 $\mu$  “hole”; 2 $\mu$  CO<sub>2</sub>; 1.5 $\mu$  OH; 1.27 $\mu$  O<sub>2</sub>; 1.0 $\mu$ )

All photodiode detectors cooled (below -100C) before flight, with sufficient

heat capacity to maintain temperature for the next 40 seconds

InGaAs, and HgCdTe photodiode detectors

Inputs coupled to windows with fibers:

Wavelengths <2.5 $\mu$  will use IR Silica

Wavelengths >2.5 $\mu$  will use IR Fluoride glass

Optics and filters 5mm diameter

Each detector output into individual gated integrator preamplifier, then digitized to 20 bits resolution

### **Scanning IR Spectrometer**

Modified Fastie-Ebert optical design, 300mm focal length

Dual spectrometer input slits coupled to windows with IR Fluoride glass fibers

Fast scan, ~0.5 second

~1.0 - 3.0 $\mu$  wavelength coverage

~0.05 $\mu$  resolution

Cooled (< -100C), photodiode detector array

Eight elements in each of two detector arrays

Photodiode types matched to specific wavelength region covered for best signal to noise

InGaAs for shortest wavelength region

Extended InGaAs (types 1-3) for intermediate regions

Photovoltaic, shortwavelength (1-3 $\mu$ ), HgCdTe for longest wavelength region

Fast (f/0.5) relay lens system at exit slit for minimum detector size

Each detector output into individual gated integrator preamplifier, then digitized to 20 bits resolution

Innovations in Multi-spectral Self-induced Shock-layer  
Radiance Measurement, Instrumentation, and Data Acquisition Suite

Clifton B. Phillips \*  
Space and Naval Warfare Systems Center  
San Diego, CA 92152-5001

Peter W. Erdman†  
Embry-Riddle Aeronautical University  
Daytona Beach, FL 32114

L. Carl Howlett‡  
Space Dynamics Laboratory  
Utah State University  
Logan, UT 84322-4140

Deborah A. Levin§  
Pennsylvania State University

Michael G. Lovern¶  
Space and Naval Warfare Systems Center  
San Diego, CA 92152-5001

David M. Mann#  
Army Research Office  
Research Triangle Park, NC 27709-2211

Abstract

Current and planned ground-based Ballistic Missile Defense (BMD) systems rely on an optical based interceptor to impact an incoming warhead. For success, the interceptor must acquire and track the target object, and then carry out maneuvers required for intercept. A main component of the target acquisition and tracking system suite is the optical sensor(s). Future missile interceptors are projected to fly at hypersonic velocities and will be expected to acquire and track the threat while

traveling within the atmosphere. An interceptor traveling at hypersonic Mach numbers will experience aerodynamic heat loading that increases temperatures on external surfaces; including optical windows. Further, thermal excitation of species occurs in the flow-field around the interceptor. Emissions from hot optics and/or excited constituents in the sensor's field of regard can lead to sensor blinding in some regions of the spectrum. The Dual-mode Experiment on Bow-shock Interactions (DEBI) project is

---

\* Technology Agent, AIAA member

† Professor, Department of Physical Science, AIAA member

‡ Technical Program Manager, Center for Space Engineering, AIAA member

§ Associate Professor, Department of Aerospace Engineering, AIAA senior member

¶ Innovative Science and Technology Program Technology Agent, AIAA member

# Associate Director, Engineering Sciences Division, AIAA Associate Fellow

This paper is in part a work of the U.S. Government and to that extent is not subjected to copyright protection in the United States.

designed to contribute further understanding toward the aerothermochemistry associated with hypersonic flight for interceptor applications within the Earth's atmosphere. Such detailed understanding is required to accurately model the optical radiation from high temperature flows. It is necessary to acquire dual-mode (ultraviolet and infrared) data during the mission flight to improve and/or validate state-of-art models developed under Ballistic Missile Defense Organization's (BMDO) Innovative Science and Technology Program. This paper summarizes the innovative solutions derived from lessons learned from the design and development of the DEBI instrumentation suite. Problems addressed were: (1) how to best detect and transport signals predicted in the short wave and mid wave infrared spectrum; (2) what detectors and wavelengths are best suited to optics constraints; (3) what new materials were necessary to improve signal to noise for a sensible acquisition system; and (4) how to design an optical payload that can perform as required in a harsh environment. Ultimately, the intention of this work is to provide BMD engineers and scientist the predictive capability necessary to design sensor systems that will be effective under flight conditions.

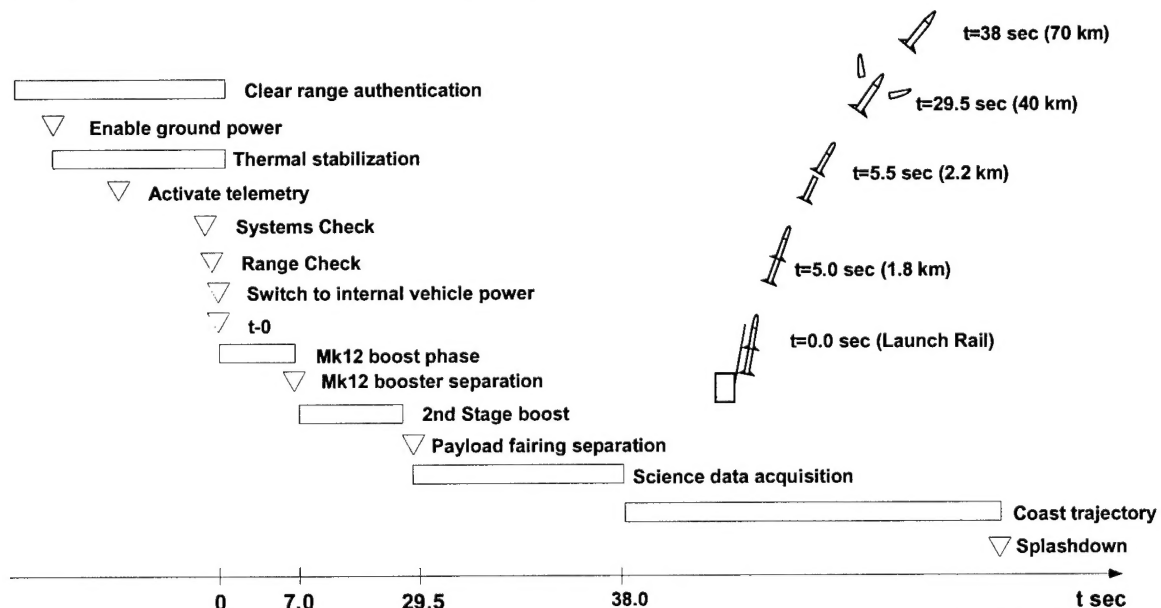
### Introduction

Current and planned ground-based BMD systems rely on optical seekers with a hit-to-kill (HTK)



Figure 1. Illustration of in-flight hypervelocity induced bow-shock on nose of the DEBI experimental vehicle.

strategy or blast fragmentation warhead to impact the incoming warhead. For this, the kinetic kill vehicle (KKV) must sense and track the target candidate and carry out the maneuvers required for the HTK intercept. For endo-atmospheric interceptors flying at hypersonic velocities the aerodynamic heating loads will significantly increase temperatures on external surfaces, including optical windows. Further, thermal excitation of species occurs in the flow field around the KKV. Given that these interceptors operate in the infrared spectrum, emissions from hot optics and/or excited constituents in the





sensor's field of regard could lead to sensor blinding in some regions of the spectrum. The DEBI program is designed to further the understanding of chemistry associated with hypersonic flight in interceptor applications within the Earth's atmosphere. The DEBI measurements are intended to examine atmospheric emissions in the shock-heated air and not aperture window emissions. Dual mode sensing (Ultraviolet and Infrared) will be employed and the data obtained in the flight test will be used to improve and/or validate state-of-art models developed under the Innovative Science and Technology program. Reference [1] describes the operational context for a two color MWIR/UV-Visible seeker. Ultimately, the program should provide BMDO the predictive capability necessary to design sensor systems that will be effective under real flight conditions.

#### Mission Operations

The DEBI experiment duration is estimated to be approximately forty seconds. The experiment delivery begins from the launch site at NASA's Wallops Island Flight facility (NASA/WFF). The experimental vehicle design reference requirement is to reach an altitude of 40 km with upward velocity of 3.5 km/s. In-flight data is to be acquired as the payload ascends and commences at 40 km following payload nose cone separation and continues through 70 km altitude. A Terrier-Malemute launch vehicle with MK-12 Terrier motor was determined to provide sufficient delta V to meet the experiment requirements on ascent. Figure 2 depicts the typical mission operations for the DEBI flight on the NASA/WFF range.

#### Science

As stated above, an overall goal of the IS&T program is to provide the predictive capability necessary for BMDO to design and deploy effective sensor systems for target acquisition and tracking in future atmospheric interceptor systems. The major goal of the DEBI flight is to characterize the outboard optical environment associated with the flight of a hypersonic interceptor in the atmospheric phase of flight. Higher speed window and sensor environments have not been spectrally characterized in controlled, flight conditions. The DEBI flight provides this opportunity. DEBI is the third in a series of sounding rocket flights. The first two

missions, Bow-shock I and Bow-shock II, focused on the Ultraviolet (UV) region of the spectrum and successfully provided data needed to improve predictive capabilities in UV wavelengths by four orders of magnitude. DEBI will focus on the Infrared (IR) region of the spectrum [2] and employ a suite of instruments to provide data on flow-field chemistry from the mid-to near-IR in the altitude range of interest (approximately 40 to 70 km) and at a representative nominal hypervelocity of 3.5 km/s. These data will then be used to refine the aerothermochemical models. UV instruments will also be used to obtain anchoring data for comparison with previous flights. The use of both UV and IR instruments also fulfills the secondary objective of demonstrating a dual mode system as a possible solution to potential sensor blinding issues. The flight will provide compelling evidence to demonstrate whether a UV seeker onboard a slender-shaped vehicle will experience any shock-layer interference or window heating problems. Unlike the IR, it is anticipated from pre-flight calculations that the window will remain transmissive in the UV and the shocklayer radiance will be below the detectivity limits of a UV instrument. For the experiment, the forebody design will be similar to that currently used in

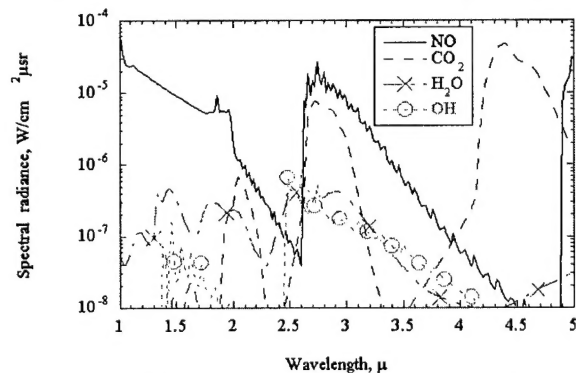


*Figure 3. IS&T aerothermochemistry model predicted response intensities for measurable species at 40 km altitude from induced bow-shock excitation at 3.5km/s.*

BMDO's Atmospheric Interceptor Technology (AIT) program to assure data is obtained with a relevant configuration. Figure 3 shows the pre-flight predicted intensities for molecular spectra excited by the bow-shock at 3.5 km/s speed and 40 km altitude. The flight data verify both the

magnitudes and spectral features shown in Figure 3. Based on our experience with earlier flight experiments we expect that there could be important differences in both predicted signal levels as well as radiating species. The species presently modeled are idealistic in that they represent IR emitting species formed by reactions of shock heated air ( $N_2$ ,  $O_2$ ,  $O$ ,  $NO$ ,  $NO_2$ ,  $CO_2$ ,  $H_2O$ ,  $OH$ ) only. Detectors covering a wide spectrum of measurements are described in the instrumentation section. Note that a few of the selected detectors correspond to peaks and valleys of the species shown in Figure 3. IR performance is expected to degrade during vehicle ascent to higher altitudes as aerodynamic heating occurs at the apertures. Full details about the predictions can be found in reference [2].

#### Instrumentation

The instruments were designed and are being fabricating three separate instrument packages for the DEBI experimental flight. The instrument packages consists of detectors imbedded within a radiometer, a spectrometer, and two UV photometers. The detectors are interconnected VIA fiber optic bundles to apertures positioned at the vehicle stagnation point and two symmetrically aft-stationed points downstream of the vehicle nose. Data to be acquired are collected from 16 scanning spectrometer channels; 2 UV channels, 6 short wave infrared (SWIR) channels, 8 mid-wave infrared (MWIR) channels, and an array of temperature sensors. Two additional data channels in the IR radiometer are dedicated to determining the MWIR detector background and the payload system noise levels. The UV detectors provide legacy data to Bow-shock I and II (BSUV 1 and 2) experimental flights.

The payload nose tip for the DEBI vehicle is illustrated in Figure 4. This design was chosen to be representative of the atmospheric interceptor technology (AIT) program so that data collected will be representative of interceptor flight. Each measurement location on the nose cone tip is fitted with a recessed sapphire lens connected to a fiber optic bundle. Table I summarizes the main characteristics of the flight scientific optical instrumentation. The table provides the onboard location and viewing information for each instrument as well as center wavelength and optical bandpass. Significant detector features and

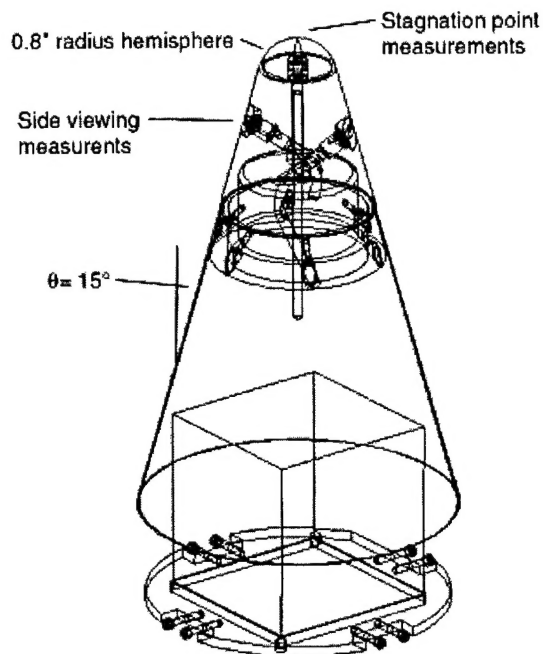


*Figure 4. Fiber optics stagnation and side view conduits positioned in DEBI payload nose tip.*

strategies as well as the intended radiating species are summarized.

DEBI UV fiber optics are well understood from previous flight experience. However, the IR fiber optic bundles provided a challenge to the design and fabrication of the DEBI payload. The primary technical problem was in selecting the appropriate fiber optics materials that met our link budgets and could also survive the environments induced from the flight and detector thermal requirements. Previous ultraviolet experience did not have an efficient carry-over into the infrared portions of the spectrum. DEBI planned for two severe environmental factors. The first environmental threat is thermal cycling during ground segment integration and checkout. During chill-down cycles there is high likelihood for direct liquid nitrogen ( $LN_2$ ) coolant contact with some instrumentation components and the fiber bundles. The other environmental concern was the acoustic-vibration flight environment. We selected fluoride glass fibers to meet all our IR requirements and used UV grade quartz fibers for the UV data channels. There was a trade off in the selection of the fluoride glass fiber material. The fluoride glass fibers were more brittle than the fiber optic materials used in Bow-shock I and



*Table 1. Summary of onboard science instrumentation.*

Meas. #	Fiber Location at Aperture	Instrument	Spectral Character	Comments
1	Stagnation point	UV photo-multiplier	0.24 $\mu$ center wavelength 0.043 $\mu$ bandpass	CsTe photo-cathode photo-multiplier detectors operated in photon counting mode
2	Side station	UV photo-multiplier	0.24 $\mu$ center wavelength 0.043 $\mu$ bandpass	CsTe photo-cathode photo-multiplier detectors operated in photon counting mode
3 – 8	Side station	MWIR	3.0 - 4.0 $\mu$ wavelength with ~0.2 $\mu$ spacing and ~0.2 $\mu$ filter bandpass  specifically: 3.07 $\mu$ CWL 0.19 $\mu$ BP 3.21        0.2 3.43        0.19 3.64        0.17 3.80        0.18 3.93        0.16	Micro Optic Multispectral Radiometer
9	Side station	MWIR	3.45 $\mu$ center wavelength with 0.54 $\mu$ filter bandpass	Micro Optic Multispectral Radiometer
10	Side station	MWIR	4.34 $\mu$ center wavelength with 0.2 $\mu$ filter bandpass	Micro Optic Multispectral Radiometer tuned for CO <sub>2</sub>
11	Side station	SWIR	0.98 $\mu$ wavelength 0.23 $\mu$ bandwidth	Micro Optic Multispectral Radiometer
12	Side station	SWIR	1.27 $\mu$ wavelength 0.3 $\mu$ bandwidth	Micro Optic Multispectral Radiometer tuned for O <sub>2</sub>
13	Side station	SWIR	1.54 $\mu$ wavelength 0.35 $\mu$ bandwidth	Micro Optic Multispectral Radiometer tuned for OH
14	Side station	SWIR	1.9 $\mu$ wavelength 0.4 $\mu$ bandwidth	Micro Optic Multispectral Radiometer tuned for CO <sub>2</sub>

*Table 1 (continued). Summary of onboard science instrumentation.*

15	Side station	SWIR	2.3 $\mu$ wavelength 0.064 $\mu$ bandwidth	Micro Optic Multispectral Radiometer tuned for predicted window
16	Side station	SWIR	2.7 $\mu$ wavelength 0.25 $\mu$ bandwidth	Micro Optic Multispectral Radiometer tuned for CO <sub>2</sub> and NO
17 - 24	Stagnation point	Scanning IR spectrometer	1.0 - 3.0 $\mu$ wavelength	500Å bandpass
25 - 32	Side station	Scanning IR spectrometer	1.0 - 3.0 $\mu$ wavelength	500Å bandpass
33 - N	N/A	Temperature	N/A	Resistive temperature elements

Bow-shock II. Consequently, the fluoride fiber material did not have a tight bend radius, which in turn created major design constraints with regard to the positions and orientations of the instrument packages. Figure 5 shows a computer aided design model showing the fiber optic connections between the stagnation and side looking apertures and the appropriate detectors within the radiometer, spectrometer, and UV detectors. Notice that in Figure 5 the radiometer is positioned two decks above the spectrometer. This resulting radiometer position was primarily to accommodate having acceptable bending radii. We benefited

form the ability to satisfy optical fiber long radius constraints and improve vehicle stability by moving the center of gravity forward. To reduce the risk of IR fiber optic breakage during flight or during handling, pre-bends were designed and fabricated into the fiber bundle harnesses. Handling is being kept to a minimum.

The UV detectors provide legacy data because they overlap with the Bow-Shock I and Bow-Shock II experimental flights. One special feature of the DEBI UV instruments is that they are designed to measure very low intensities in side-viewing direction.

The MWIR and SWIR radiometers have InGaAs and HgCdTe photodiode detectors coupled to windows with IR fluoride glass fibers. The scanning infrared (IR) spectrometer has a fast f/0.5 relay lens system at the exit slit and a stepper motor driven diffraction grating with InGaAs photodiode detectors for short wavelength regions, extended InGaAs photodiode detectors for the intermediate wavelength regions, and photo-voltaic short wavelength HgCdTe detectors for longest wavelength regions. When our team received the detectors they were configured differently than what was expected. Procurement was not an option because of long lead times associated with the small quantity used in the DEBI experiment. This made necessary a modification to focus the appropriate amount of energy upon the detectors as received. We engineered a system of lenses to solve this problem. One key element used to get an acceptable signal to noise ratio for the MWIR was

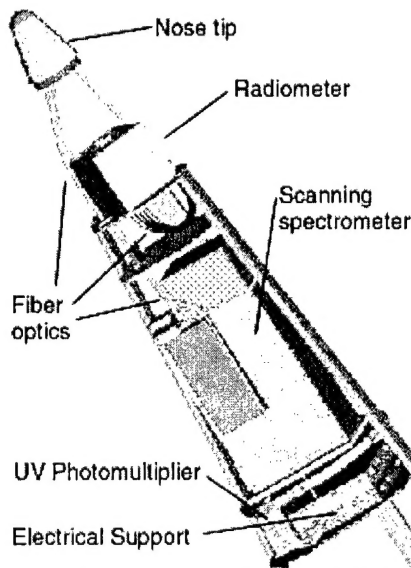


*Figure 5. Rendering of CAD model showing fibers connecting the stagnation point and side looking directions to appropriate instruments using long radii bends.*

the implementation of chalcogenide glass for a lens material. The chalcogenide material has a low index of refraction, was readily available, and easily machined by skilled lens makers. Consequently the chalcogenide glass material made it possible to get an appreciable amount of light upon the MWIR detectors to meet acceptable expected signal to noise ratios (SNR) for the detector material. All detectors will be cooled below 193K before flight and provided with sufficient thermal inertia to maintain acceptable temperature limits for the in-flight 40 second duration

#### Payload

Payload elements include structures, thermal control, power, telemetry, command and data handling, and the payload fairing. The payload subsystem is built with the requirement instruments survive the stressful flight experience sufficiently long to satisfy the science objectives to collect data over as large an altitude range as possible. The integration of instruments into a payload must provide a cold environment for the IR instruments, fiber optics and nose tip and an even colder environment for the detectors themselves while providing a warm environment for the all the rest of the payload electronics. It must protect this internal environment from the extremely severe aeroheating in the dense atmosphere to point at 40 km when the rocket motor burns to completion and the velocity is 3.5 km/s. At this time we require a chemically clean and cold measurement surface of desired shape to be presented to the flow field. The measurement nose tip is designed to not allow black body radiation from the from the tip itself to enter the fiber optics until the payload reaches an altitude of approximately 70 km. An entire section of the payload including the nose tip will be isolated from the rest of the payload and the outside environment and kept at a temperature of approximately  $-60^{\circ}\text{C}$ . An ejection clam shell nose cone will provide protection for the cold section from the extreme ascent aeroheating.

The measurement surface will be quickly heated after the clam shell nose is ejected. It should be noted that copper is used for the forward hemispherical surface to absorb the strong heat flux without getting so hot its black body radiation will mask the atmospheric radiation to be measured. Another key to preventing this

interference is to use a cold sapphire lens to image the end of the fiber bundle to a location outside of the nose tip. The fiber bundle and lens are recessed within the nose tip and will be slow to heat. The aperture that they view through is kept outside of the optical field of view. At least one scatter is required for black body radiation to enter the measurement system.

#### Ejection Nose Cone

The ejection nose cone design is very critical to the success of the DEBI program. There are several difficult requirements that must be met that are entirely unique to DEBI that did not exist on the related Bow-shock 1 (BSUV 1) program. They are as follows:

1. Meet the demanding thermal constraints of allowing the coldest part of the payload to remain cold and still be within inches of the nose cone ejection electronics that must remain warm. The thermal separation must be done without compromising the ability to separate the nose cone halves and without vacuum jackets and MLI to provide insulation.
2. Maintain a dry environment so that frost does not form on optical surfaces prior to launch.
3. Maintain protection from optical system frosting during the early stages of flight when the dynamic pressure on the outside of the nose cone is greater than the ambient pressure inside the inside. During these conditions, the direction of flow of warm moist Virginia night air will be inward toward the very cold nose tip optics.

In order to meet the thermal requirements, the cold inner nose cone is separated from the outer stainless steel skin by a fiberglass inner shell. The photograph in Figure 7 shows the inner nose cone tip fitted within half the nose cone shell. The shell is built in two halves mounted to the stainless steel skin. The gap between the fiberglass shield and the stainless skin is filled with fiberglass building insulation. This relatively low-tech material was chosen because there are no significant trapped air spaces to retain moisture like are present within foams. It will be a material that is less difficult to purge than other options even though there are better insulators.

The separation v-joint at the base of the cone is mated to a steel ring at the top of the carbon fiber skin. Since it is in the cold section, it will be at or near the  $-60^{\circ}\text{C}$  temperature. The section of the ejection nose cone forward of the fiberglass shell needs to be near ambient temperature for the proper operation of the ejection electronics. This is accomplished through thermal conduction from the surrounding air outside of the nose cone, warming the cone and its contents. The aft section of the ejection nose cone which can and will be cold is covered by an external foam insulator, which will be torn away upon liftoff. Approximately a  $80^{\circ}\text{C}$  temperature differential will need to be maintained across the aft 15 inches or so of the stainless steel cone without producing a lot of frost or ice forward of the insulation. The external foam insulator seemed to work satisfactorily during early testing without the ablative since the stainless steel nose tip material

is a poor thermal conductor.

In order to minimize the infiltration of hot air into the ejection nose cone during flight, we have gone to considerable care to make certain that the nose cone halves fit together very well. In quantitative terms, that means that there should be no gap wider than .005 inches. A narrow gap is good from the standpoint of moist air infiltration into the nose cone during flight, but is just as bad with respect to purging of moisture trapped inside prior to flight. There are some tradeoffs that will have to be examined during integration testing to be certain that the purge is sufficient without making the cone excessively leaky during flight.

The tight fit between cone halves was obtained by placing one of the cone halves on a flat surface covered with a release film to which epoxy does not bond. An epoxy-quartz microsphere mixture was applied to the edges of the cone and the cone

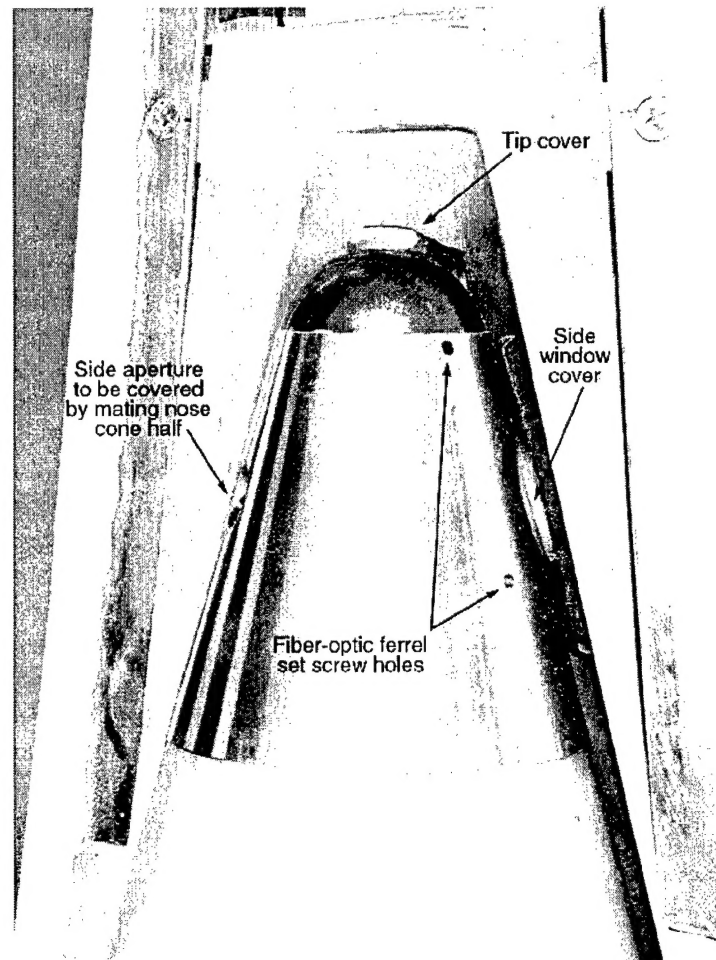


Figure 7. DEBI nose tip showing half of the ejection cover and aperture covers.

was then placed on the flat release film. When cured, this makes a precision flat surface. The cone half was removed from the release film and a layer of release film was applied to the new flat surface. Epoxy-microsphere mixture was applied to the other nose cone half and the two were bolted together. This produces an exactly mating surface between the two halves. After the two halves have cured, the assembled nose cone is coated with the ablative material to protect against the extreme aerodynamic heating upon ascent. After the ablative has cured, the two halves can be separated and the ablative trimmed. Since the glass-epoxy mixture used to achieve the precision joint cannot stand high temperatures, it relies on the ablative for protection during flight. An access door for pyrotechnic installation, the electrical umbilical and purge gas umbilical provided additional ablative application complications but seem to have worked out quite well.

The ablative is a polyurethane material which was selected because of its low activation temperature. When it has cured, it is quite soft, yet cuts and sands freely. When it bends it takes a moderate amount of force to make the bend but when the force is released it relaxes slowly. It should be an outstanding vibration dampening material unless its properties change dramatically with temperature. When subjected to heat from a welding torch, the ablative surface melts and evaporates keeping the inner surface below the activation temperature.

Figure 7 also shows graphite spring loaded covers over each aperture prior to nose tip ejection. These covers are required to prevent frost from forming upon the cold optical surfaces. Each cover has a sapphire window to allow instrument testing prior to the beginning of the in-flight measurement period. A grain of wheat incandescent light bulb is included in the fiberglass inner shell and powered through the nose cone umbilical to provide a means of testing the instrumentation prior to flight.

The split line in the nose cone was intentionally indexed to the payload body so that it does not line up with either of the side view apertures. The forward viewing instrument however, will look directly into the split between the two fiberglass shells. It will certainly see

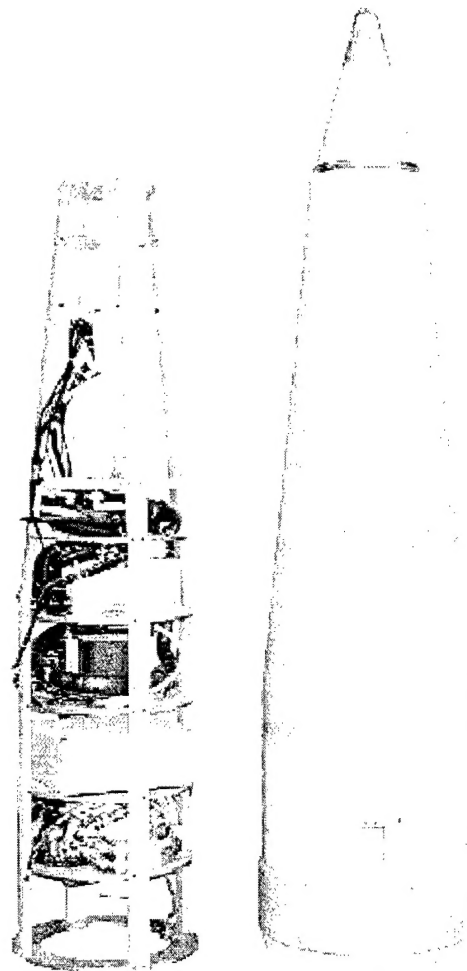


*Figure 8. Polyurethane coated nose section and payload skins stacked next to structure and housekeeping components.*

black body radiation of unpredictable magnitude that will likely be different in flight than with either no outside lighting on the payload or with the possibility of light-leaked outside illumination. We will choose the most beneficial cover/window option during payload integration and testing.

Figure 8 shows the entire stack next to the external appearance of the skin and nose tip section. Figure 9 shows the entire view of the split nose fairing to be jettisoned in flight. Figure 10 identifies the major section of the payload. The instruments are not shown in Figure 10. However, their locations are apparent by comparing Figure 6 to Figure 5 to Figure 10.

### Delivery Vehicle

The DEBI experiment will be launched on a Terrier-Malemute launch vehicle from NASA/Wallops Flight Facility (WFF). The flight vehicle ignition deck was modified with Government furnished transponder, transmitter, timers and a

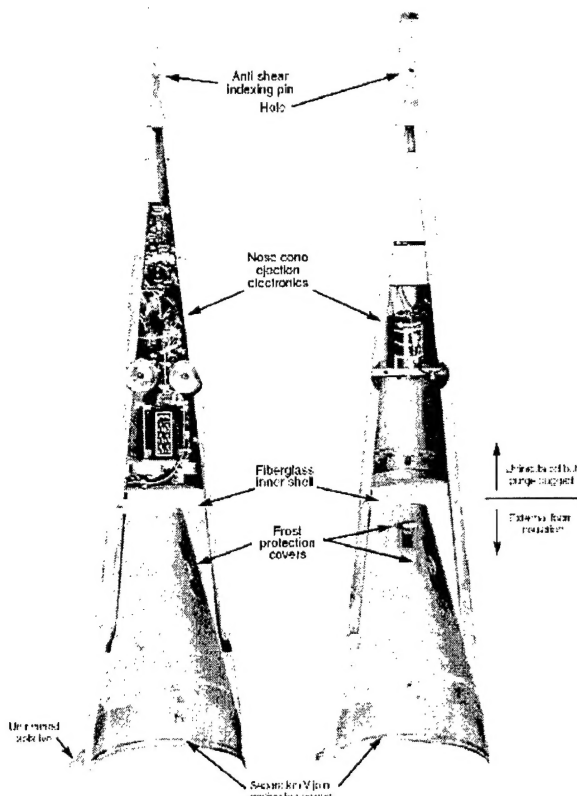


Figure 9. DEBI ejection nose cone.

Malemute ignition deck in the payload compartment. Installation of components onto the ignition deck plate occurred at WFF. The completed ignition deck plate is now integrated into the payload.

### Conclusion

Several issues of concern for capturing in-flight data in the MWIR and SWIR portions of the spectrum data have been identified for those who plan to implement operational missions or experiments within this regime. We implemented solutions through design and materials selection for many of the issues identified. In addition to the scientific data, an important outcome of this flight will be the validation of our engineering

solutions for small, affordable rocket flight experiments.

### Acknowledgements

The DEBI project is a result of teamwork. This work is sponsored by Dr. Juergen Pohlmann, director of the Ballistic Missile Defense Innovative Science and Technology (IS&T) Program. Embry Riddle Aeronautical University (ERAU) in Daytona Beach Florida designed and is fabricating three separate instrument packages for the DEBI experimental flight. The payload bus, nose tip, and ejection system is designed and fabricated by Space Dynamics Laboratory (SDL) at Utah State University. Science team members from Pennsylvania State University (PSU) provided the pre-flight spectral and radiometric calculations. The terrier-malamute and respective launch and range services were procured from the NASA Wallops Flight Facility (NASA/WFF) were engineers designed and built the boost vehicle ignition deck. The Instrument portion is executed from Army Research Office. The DEBI payload is executed from the Space and Naval Warfare Systems Center in San Diego California.

### References

- 1 D. Levin, D. Mann, C. Phillips, M. Lovern, C. Howlett, "Multi-spectral shocklayer radiance measurement plan and predictions for the DEBI flight experiment," 8th Annual AIAA /BMDO conference, MIT Lincoln Laboratory, 19-22 July, 1999.
- 2 D. Levin, G. Candler, C. Limbaugh, "Multi-spectral Shocklayer Radiation from a Hypersonic Slender Body," AIAA Paper No. 99-3747, 33rd Thermophysics Conference, Norfolk VA, 28 Jun - 1 July 1999.
- 3 P. W. Erdman, E. C. Zipf, P. Espy, C. Howlett, D. A. Levin, R. J. Collins, and G. V. Chandler, "Measurements of Ultraviolet Radiation from a 5 km/sec Bow Shock," Journal of Thermalphysics and Heat Transfer, 8, 441, 1994.
- 4 P. W. Erdman, E. C. Zipf, P. Espy, C. Howlett, D. A. Levin, R. Loda, R. J. Collins, and G. V. Chandler, "Flight Measurements of Low Velocity Bow Shock Ultraviolet Radiation," Journal of Thermalphysics and Heat Transfer, 7, 37, 1993.



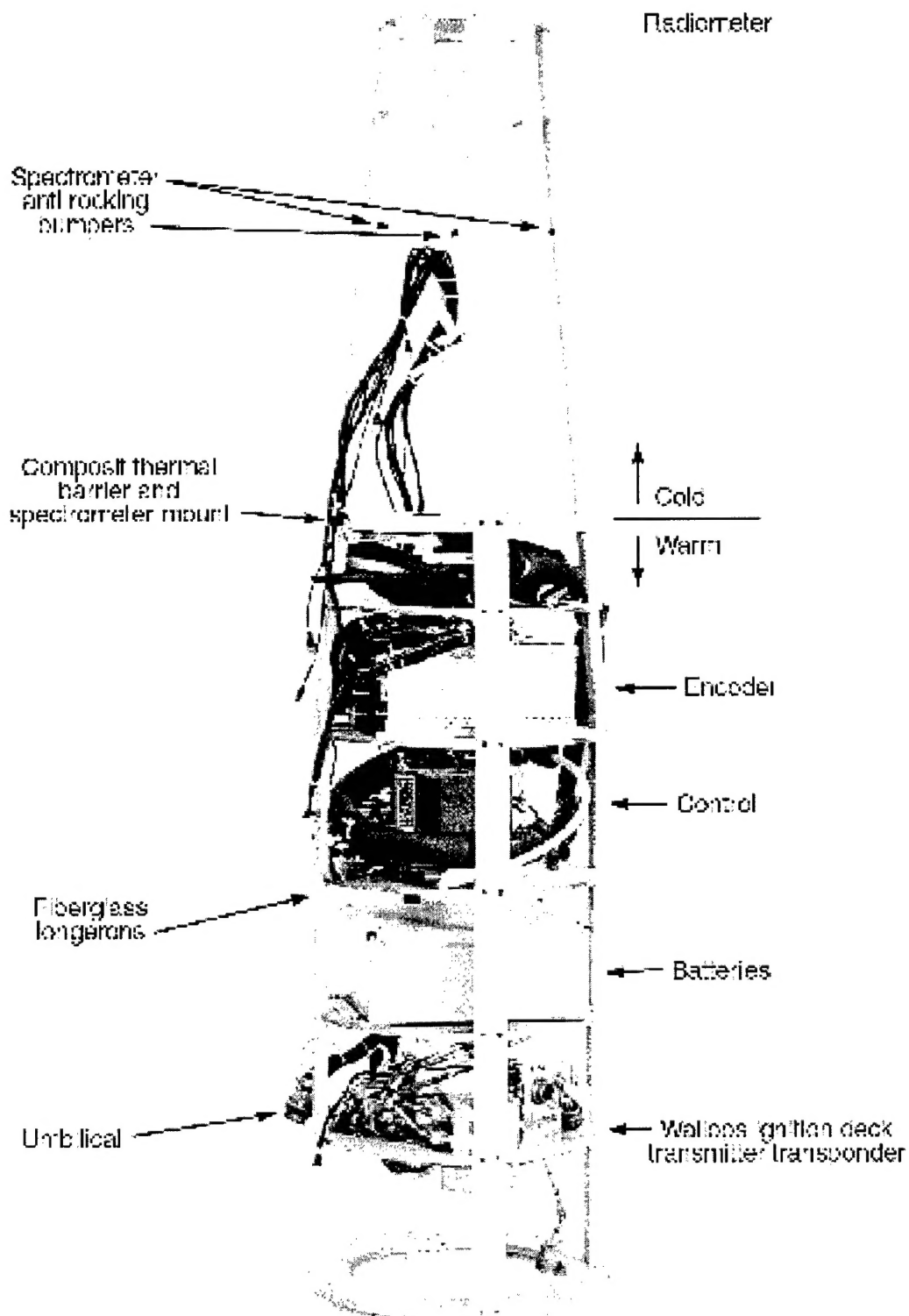


Figure 10. Payload structure, house keeping and communication, command, and control components.